

1 **Record-low Arctic stratospheric ozone in 2020: MLS**  
2 **observations of chemical processes and comparisons**  
3 **with previous extreme winters**

4 **Gloria L Manney<sup>1,2</sup>, Nathaniel J Livesey<sup>3</sup>, Michelle L Santee<sup>3</sup>, Lucien**  
5 **Froidevaux<sup>3</sup>, Alyn Lambert<sup>3</sup>, Zachary D Lawrence<sup>4,1</sup>, Luis F Millán<sup>3</sup>, Jessica L**  
6 **Neu<sup>3</sup>, William G Read<sup>3</sup>, Michael J Schwartz<sup>3</sup>, Ryan A Fuller<sup>3</sup>**

7 <sup>1</sup>NorthWest Research Associates, Socorro, NM, USA

8 <sup>2</sup>New Mexico Institute of Mining and technology, Socorro, NM, USA

9 <sup>3</sup>Jet Propulsion Laboratory, California Institute of Technology, Pasadena, CA, USA

10 <sup>4</sup>National Oceanic and Atmospheric Administration / Cooperative Institute for Research in  
11 Environmental Sciences, Boulder, CO, USA

12 **Key Points:**

- 13 • MLS trace gas data show that exceptional polar vortex conditions led to record-
- 14 low ozone in the Arctic lower stratosphere in 2019/2020
- 15 • Early and persistent cold conditions led to the longest period with chlorine in ozone-
- 16 destroying forms in the 16-year MLS data record
- 17 • Chemical ozone destruction began earlier than in any Arctic winter in the MLS
- 18 record and ended later than in any year except 2010/2011

---

Corresponding author: Gloria L Manney, [manney@nwra.com](mailto:manney@nwra.com)

**Abstract**

Aura Microwave Limb Sounder (MLS) measurements show that chemical processing was critical to the observed record-low Arctic stratospheric ozone in spring 2020. The 16-year MLS record indicates more polar denitrification and dehydration in 2019/2020 than in any Arctic winter except 2015/2016. Chlorine activation and ozone depletion began earlier than in any previously observed winter, with evidence of chemical ozone loss starting in November. Active chlorine then persisted as late into spring as it did in 2011. Empirical estimates suggest maximum chemical ozone losses near 2.8 ppmv by late March in both 2011 and 2020. However, peak chlorine activation, and thus peak ozone loss, occurred at lower altitudes in 2020 than in 2011, leading to the lowest ozone values ever observed at potential temperature levels from  $\sim 400$ – $480$  K, with similar ozone values to those in 2011 at higher levels.

**Plain Language Summary**

Unlike the Antarctic, the Arctic does not usually experience an ozone hole because temperatures are often too high for the chemistry that destroys ozone. In 2019/2020, satellite measurements show record-low stratospheric wintertime temperatures and record-low springtime ozone concentrations in the Arctic lower stratosphere (about 12–20 km altitude). Only one other winter/spring season, 2010/2011, in this 16-year satellite data record comes close. Low temperatures, which result in chlorine being converted from non-reactive forms into forms that destroy ozone, started earlier than in any previous Arctic winter in the record and lingered later than in any year except 2011. The ozone-destroying chemistry in 2019/2020 occurred at lower altitudes (where more of the ozone that filters out harmful ultraviolet radiation resides) than in 2010/2011. Such extensive ozone loss can have important health and biological impacts because it leads to more ultraviolet radiation reaching the Earth’s surface. While the success of the Montreal Protocol in limiting human emissions that increase ozone-destroying gases in the stratosphere has resulted in much less Arctic ozone destruction than we would have otherwise had, future temperature changes could lead to other winters with even more chemical ozone depletion than in 2019/2020.

**1 Introduction**

Arctic chemical ozone loss varies dramatically because of extreme interannual variations in the meteorology of the stratospheric polar vortex (e.g. WMO, 2014). For the past 16 years, the Aura Microwave Limb Sounder (MLS) has been providing a uniquely comprehensive suite of daily global measurements of species involved in lower stratospheric polar chemical processing. The two previous Arctic winters on record with coldest conditions and greatest ozone loss occurred during this period: In 2010/2011, although lower stratospheric minimum temperatures did not consistently set records, the exceptionally prolonged (lasting into April) cold led to unprecedented Arctic chemical ozone loss (Manney et al., 2011; WMO, 2014, and references therein). December 2015–January 2016 Arctic temperatures were the lowest in at least 68 years (Manney & Lawrence, 2016; Matthias et al., 2016), Arctic denitrification and dehydration were the most severe in the MLS record (e.g., Manney & Lawrence, 2016; Khosrawi et al., 2017), and ozone dropped more rapidly than in 2010/2011. Springtime cumulative ozone loss did not match or surpass that in 2011 only because a major final warming in early March 2016 halted chemical processing and dispersed processed air from the vortex (Manney & Lawrence, 2016; Johansson et al., 2019). In 2019/2020, lower stratospheric temperatures were persistently below the threshold for chemical processing on polar stratospheric clouds (PSCs) and other aerosols earlier than in any other year observed by MLS and remained low approximately as late as in 2011 (see Lawrence et al., 2020, for an overview of stratospheric vortex meteorology in 2019/2020).

We use the MLS version 4 dataset (Livesey et al., 2020), along with meteorological fields from the Modern Era Retrospective Analysis for Research and Applications Version 2 (MERRA-2) (Gelaro et al., 2017) to show details of lower stratospheric polar processing in the extraordinary 2019/2020 winter/spring Arctic vortex, the resulting record-low ozone values, and comparisons with the previous Arctic winters (2010/2011 and 2015/2016) during which MLS observed largest ozone losses.

## 2 Results

Figures 1a–g show Northern Hemisphere (NH) MLS 520 K ( $\sim 18$  km) trace gas maps in December 2010, 2015, and 2019.  $\text{N}_2\text{O}$  within the polar vortex was substantially lower (and  $\text{H}_2\text{O}$  higher) by early December 2020 than that in either 2015 or 2010, and its gradients across the vortex edge were steeper, consistent with a stronger signature of confined descent and/or descent of lower values from above. By 9 December, the region of temperatures below the nitric acid trihydrate (NAT) PSC threshold (Hanson & Mauersberger, 1988) was larger and more concentric with the vortex in 2019 and 2015 than in 2010. Temperatures remained consistently below this threshold starting earlier in 2019 (by mid-November) than in either 2010 (which did not become cold particularly early) and 2015 (which did) (see Lawrence et al., 2020, to be submitted). Both 2019 and 2015 showed significant areas of depressed  $\text{HNO}_3$  in the vortex by 9 December, but only 2019 showed substantial chlorine activation; in fact, much of the sunlit portion of the vortex was filled with high  $\text{ClO}$  by 1 December 2019, with a corresponding region of low  $\text{HCl}$  values. Typically, lower stratospheric ozone ( $\text{O}_3$ ) is higher near the vortex edge than in its core before the onset of chemical loss and increases through late December (as in 2015 and 2010). In 2019, however,  $\text{O}_3$  was already lower throughout the vortex (even near the inside edge) than outside by 1 December and continued to decline through the month, while it continued increasing outside the vortex as in other years. Along with the early chlorine activation, this suggests a very early onset of chemical  $\text{O}_3$  loss.

Figures 1h–n show 460 K ( $\sim 16$  km) maps on dates when each species is near its most extreme observed values in the polar vortex. By 26 March 2020,  $\text{N}_2\text{O}$  throughout the vortex was even lower compared to other years (and  $\text{H}_2\text{O}$  in the portions unaffected by ice PSCs was higher) than in December, consistent with the signature of confined descent continuing to be unusually strong. The depression in  $\text{HNO}_3$  abundances, evident in large portions of the vortex in each winter shown, was more severe in 2020. In contrast, temperatures remained below the ice PSC threshold much longer in 2016 than in any other Arctic winter on record (Manney & Lawrence, 2016; Matthias et al., 2016), leading to unprecedented dehydration (Khosrawi et al., 2017). Through most of the winter (e.g., Fig. 1k),  $\text{HCl}$  was slightly lower in 2020 than in 2011, and lower in both of those years than in 2016; consistent with this, on the same dates  $\text{ClO}$  was comparably high in 2020 and 2011, and somewhat lower in 2016. MLS recorded no data from 27 March through 19 April 2011 because of an instrument anomaly (e.g. Manney et al., 2011). By 26 March (Fig. 1m), 460 K  $\text{O}_3$  was distinctly lower in 2020 than in 2011 and remained so until late April (Fig. 1n), when values had started to rise in both years as the vortex weakened. Maps of extreme values of trace gases on MLS retrieval levels (see supporting information, hereinafter “SI”, Figs. S1 and S2) show consistent results, with lower minimum values in 2020 than in 2011 both before and after the 2011 data gap.

Figure 2 shows 460 K MLS 2019/2020 fields along with differences from climatology for 2019/2020, 2015/2016, and 2010/2011 as a function of equivalent latitude (the latitude that would encompass the same area between it and the pole as each potential vorticity, PV, contour, Butchart & Remsberg, 1986) and time, giving a vortex-centered view of the seasonal evolution. In 2019/2020, vortex temperatures (Fig. 2a shows MERRA-2 temperatures) were comparable to those in 2010/2011 and much lower than climatological values in late February through March. During late December through January, 2015/2016 temperatures were still the lowest on record, with the longest period below

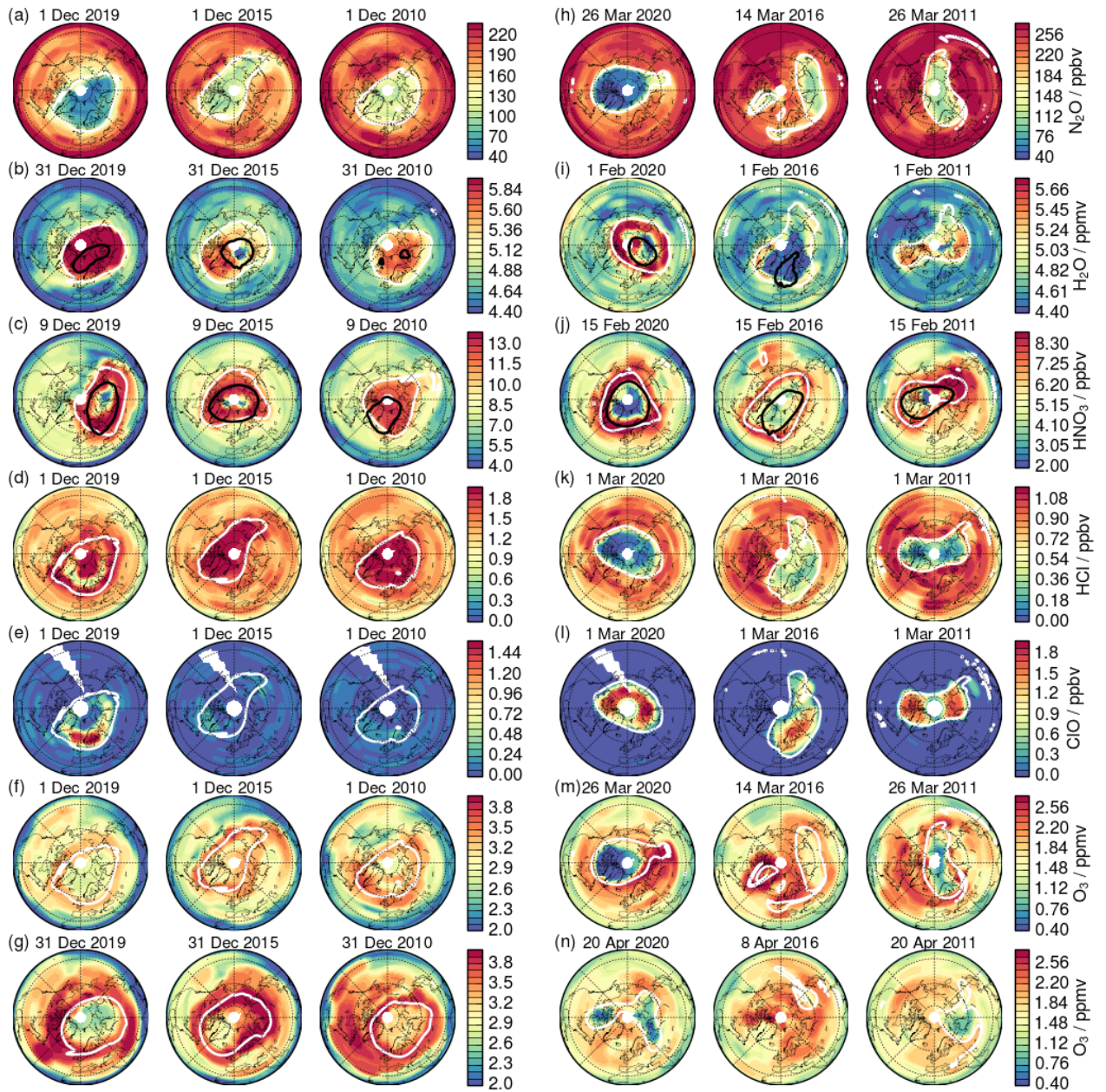


**Figure 1.** MLS maps: (a–g) 520 K in December and (h–n) at 460 K on dates illustrating extreme values, for 2019/2020, 2015/2016, 2010/2011. Overlays: vortex boundary scaled potential vorticity (sPV, white; see Lawrence et al., 2018; Lawrence & Manney, 2018); NAT (on  $\text{HNO}_3$ ) and ice (on  $\text{H}_2\text{O}$ ) PSC threshold temperatures (black). 26 March (20 April) (m–n for 2011, 2020) is the day before (day after) the 2011 data gap.

121 the ice PSC threshold (e.g., Lawrence et al., 2020); however, since low temperatures are  
122 more common during these months than later on, the 2015/2016 temperatures were not  
123 as anomalous as those later in the season in 2020 and 2011. Temperatures were anomalous  
124 low much earlier in the winter in 2019/2020 than in 2010/2011.

125 Vortex strength (Fig. 2a, MERRA-2 overlays) particularly stands out in 2019/2020  
126 (see also Lawrence et al., 2020), with PV gradient anomalies in late December 2019 com-  
127 parable to those in mid-January 2011 and much stronger PV gradient anomalies as the  
128 season progresses than those in 2011 (the previous record-strong lower stratospheric vor-  
129 tex, e.g., Manney et al., 2011; Lawrence et al., 2020). The scaled PV (sPV) overlays in  
130 Figures 2b-g also emphasize these differences and show that the 2019/2020 vortex at-  
131 tained its maximum area earlier and maintained it longer than in other years; further-  
132 more, the 2019/2020 vortex was larger than that in 2010/2011 throughout the winter.

133 Figure 2b,c shows  $\text{N}_2\text{O}$  and  $\text{H}_2\text{O}$  as the difference from each year's 1 November field  
134 to emphasize changes in the confined descent signature through the winter.  $\text{N}_2\text{O}$  decreased  
135 more rapidly through February 2020 and developed steeper gradients across the vortex  
136 edge, clearly indicating stronger and more confined vortex descent than in previous years.  
137 Before temperatures reach ice PSC thresholds,  $\text{H}_2\text{O}$  also showed this signature as a more  
138 rapid increase in 2019/2020 than in other years. Work in progress indicates that this sig-  
139 nature arises largely from a combination of descent of anomalously low  $\text{N}_2\text{O}$ /high  $\text{H}_2\text{O}$   
140 entrained into the developing mid-stratospheric vortex and stronger vortex confinement  
141 in 2019/2020 than in the other years shown.

142 Consistent with the temperature and vortex evolution, the period of low gas-phase  
143  $\text{HNO}_3$  was longest in 2019/2020: While negative  $\text{HNO}_3$  anomalies in late December 2015  
144 and January 2016 were more pronounced, and significant low anomalies lingered longer  
145 in 2011 than in 2016, in 2020 low anomalies appeared only slightly later than in 2016  
146 and endured as late as those in 2011. Moreover, since  $\text{HNO}_3$  was anomalously high be-  
147 fore the onset of PSCs in 2019/2020, the net decrease was similar to that in 2016. Sig-  
148 nificant denitrification occurred in both 2011 and 2016 (e.g., Manney et al., 2011; Khos-  
149 rawi et al., 2017; Johansson et al., 2019), and similarly low values indicate extensive den-  
150 itrification in 2020. There were several multi-day periods in 2020 with temperatures be-  
151 low the ice PSC threshold, notably in late January, and a distinct signature of  $\text{H}_2\text{O}$  se-  
152 questration in PSCs is seen in early February; this drop (considering higher  $\text{H}_2\text{O}$  values  
153 before its onset) is comparable to the initial drop in 2016. Small negative or reduced pos-  
154 itive anomalies near the vortex core persisted for a month or so after temperatures rose  
155 above the ice PSC threshold in 2020, suggesting some dehydration; however, 2016 (when  
156 strong low anomalies lingered throughout the season) remains the only Arctic winter in  
157 which MLS observed vortex-wide dehydration.

158 With few exceptions, chlorine was activated through at least late January in the  
159 Arctic winters observed by MLS.  $\text{HCl}$  (Fig. 2e) dropped to anomalously low values as  
160 soon as the vortex was well-defined in 2019/2020 and 2015/2016, whereas chlorine ac-  
161 tivation in 2010/2011 was near average until late January.  $\text{ClO}$  values (Fig. 2f) before  
162 March depend strongly on vortex size and position since much of the vortex may be in  
163 darkness; nevertheless, anomalously high  $\text{ClO}$  during most of December 2019 (compared  
164 with near-climatological values until late December in the other years) highlights early  
165 chlorine activation in 2019/2020.  $\text{ClO}$  anomalies in March were similarly high in 2020  
166 and 2011. Arctic chlorine deactivation normally proceeds through the reformation of  $\text{ClONO}_2$   
167 (e.g., Douglass et al., 1995). In all three years highlighted here, however, low- $\text{HNO}_3$ , low-  
168 ozone, and low-temperature conditions shifted deactivation towards a more Antarctic-  
169 like pathway, with rapid  $\text{HCl}$  reformation. While we do not know the exact timing of de-  
170 activation in 2011 because of the instrument anomaly, the common periods MLS observed  
171 show similar patterns in 2020 and 2011.

172 The end result of the more prolonged polar processing in 2019/2020 is apparent  
173 in  $O_3$ , with substantial low anomalies beginning in early January. Since we would expect  
174  $O_3$  to increase via descent in the strong 2019/2020 vortex, this pattern suggests ap-  
175 preciable chemical loss beginning by late November 2019. Strong low  $O_3$  anomalies are  
176 apparent after early February 2016 and after early March 2011. The lowest  $O_3$  observed  
177 in 2020 was much lower than that in 2011 at this altitude, and the larger vortex means  
178 that these low values covered a greater area. Although  $O_3$  may have continued to de-  
179 crease during the data gap in 2011, it is clear that the area of very low  $O_3$  was never com-  
180 parable to that in 2020 (consistent with area of lowest values shown in Fig. 1 and low-  
181 est minimum values Figs. S1 and S2).

182 Vortex averages of MLS data are provided in “Level 3” products that have recently  
183 been made public (Livesey et al., 2020, see SI for further description). Vortex-averaged  
184 cross-sections (Figure 3) show the vertical structure of the changes shown in Fig. 2. We  
185 focus on comparison of 2020 and 2011, since the extreme aspects of 2016 were previously  
186 discussed and those conditions did not result in springtime  $O_3$  loss comparable to that  
187 in 2020 and 2011. Strong confined descent is apparent in the  $N_2O$  and  $H_2O$  anomaly fields  
188 and in the greater convergence of the overlaid contours of the values that were at 540  
189 and 620 K on 1 November in 2020 than in 2011. The increased  $N_2O$  at the top of the  
190 2020 plot indicates the beginning of the vortex breakup at higher levels in April.

191 In 2019/2020, the area of potential PSC formation shifted steadily down through  
192 the winter, with largest areas below PSC thresholds near 520–540 K in early winter and  
193 near 460–480 K in late winter/spring; in 2010/2011, this area shifted from  $\sim$ 520 K in early  
194 winter to  $\sim$ 500 K in spring. The area of anomalously low  $HNO_3$  follows this vertical pro-  
195 gression. In 2019/2020, increasing high  $HNO_3$  anomalies in late December and January  
196 below the cold region suggest renitrification as PSCs sedimented from above evaporated;  
197 a similar pattern was seen in January 2011, albeit with smaller anomalies. High  $H_2O$  anoma-  
198 lies throughout most of 2019/2020, consistent with the strong confined descent signa-  
199 ture in  $N_2O$  discussed previously, are related to initially low/high mid-stratospheric  $N_2O/H_2O$ ;  
200 the abrupt shift from strong high anomalies to no significant anomalies in late January  
201 to early February reflects a period with substantial ice PSC activity.  $H_2O$  anomalies were  
202 weak in 2011 as ice PSCs were infrequent.

203 The patterns of chlorine activation seen in  $HCl$  and  $ClO$  are consistent with the  
204 evidence of PSC activity in temperatures and  $HNO_3$ , with the region of most depleted  
205  $HCl$  at lower altitudes in winter/spring 2019/2020 than in 2010/2011 – minimum  $HCl$   
206 values in spring 2020 end up at  $\sim$ 480 K versus  $\sim$ 520 K in 2011. During the period when  
207  $ClO$  is highest, maximum values were near 460 K throughout March 2020 and moved from  
208  $\sim$ 520 K in early March to  $\sim$ 480 K in late March in 2011. Anomalously high  $ClO$  in De-  
209 cember 2019 and early January 2020 was consistent with  $HCl$ , but varied depending on  
210 how much of the vortex experienced sunlight; in contrast,  $HCl$  in December 2010 was  
211 slightly higher than climatology, indicating a relatively late start to chlorine activation.

212 Ozone contours (Fig. 3f) show a strong downward tilt through November, consis-  
213 tent with the strong descent signature seen in  $N_2O$  and  $H_2O$ . Since  $N_2O$  and  $H_2O$  con-  
214 tours continue to indicate strong descent through December, the flattening of  $O_3$  con-  
215 tours and appearance of negative  $O_3$  anomalies suggest that chemical  $O_3$  loss began by  
216 late November and overwhelmed replenishment by descent by early December. In 2011,  
217 strong negative  $O_3$  anomalies first appeared in February. Although the MLS record in  
218 2011 is incomplete, no evidence suggests that  $O_3$  reached values as low as those in 2020.  
219 Further, minimum vortex-averaged  $O_3$  occurred near 440–460 K in 2020 but 480–500 K  
220 in 2011; thus even when values dipped as low in 2011, they were at smaller pressures and  
221 consequently affected the total column less. Record-low column ozone and associated record-  
222 high surface ultraviolet will be discussed in papers in this special collection (e.g., Bern-  
223 hard et al., 2020, in preparation).

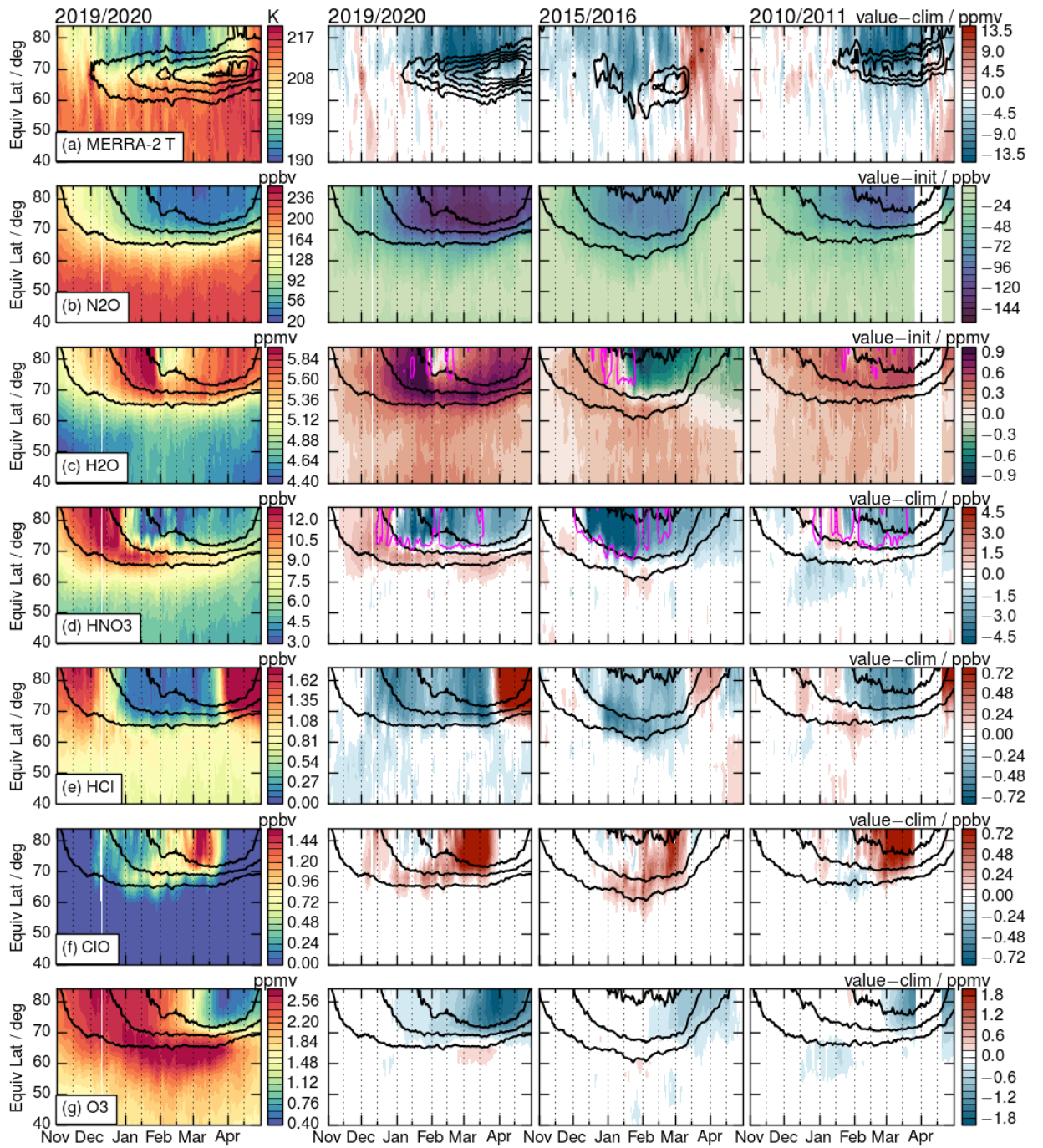


**Figure 2.** (a) 460 K EqL/time plots of MERRA-2 temperature for 2019/2020 (left), and difference from climatology for (following columns) 2019/2020, 2015/2016, and 2010/2011; overlays: sPV gradients (left) and positive sPV gradient differences from 2004/2005–2019/2020 climatology (remaining columns). (b–c) EqL/time plots of 460 K MLS  $\text{N}_2\text{O}$  and  $\text{H}_2\text{O}$  for 2019/2020 (left), and differences from the 1 November values (remaining columns). (d–g) As in (b–c), but for other MLS trace gases and differences from 2004/2005–2019/2020 climatology; overlays: vortex edge sPV (black), temperature (magenta; 197 K on  $\text{HNO}_3$ , 192 K on  $\text{H}_2\text{O}$ ).

Vortex-averaged profiles on individual days (Fig. 3, left column) quantify differences between 2020 and 2011. There was a stronger confined descent signature and evidence of more PSC activity in 2020 than in 2011. Chlorine activation was similar at lower altitudes in both years but stronger at higher altitudes in 2011. O<sub>3</sub> abundances were smaller below about 500 K in 2020 than in 2011. Supplementary Fig. S3 shows raw MLS profiles indicating that, though vortex averages were only slightly lower in 2020 than in 2011, localized minimum values were near zero in late March 2020, compared to ~0.5 ppmv in 2011, and occurred at lower altitude. Comparisons of minima from ozonesondes and MLS data (Ingo Wohltmann, personal communication) show consistent results.

Figure 3g shows chemical estimates of O<sub>3</sub> loss using the “MLS Match” method (Livesey et al., 2015, see SI for further information). The computed cumulative chemical change in 2019/2020 indicates some early chemical loss above 520 K, but largest loss between about 400 and 470 K. Similar loss rates were computed for 2020 and 2011 through late March, with maximum losses near 2.8 ppmv. However, consistent with observed chlorine activation, maximum losses were at lower altitude in 2020 than in 2011.

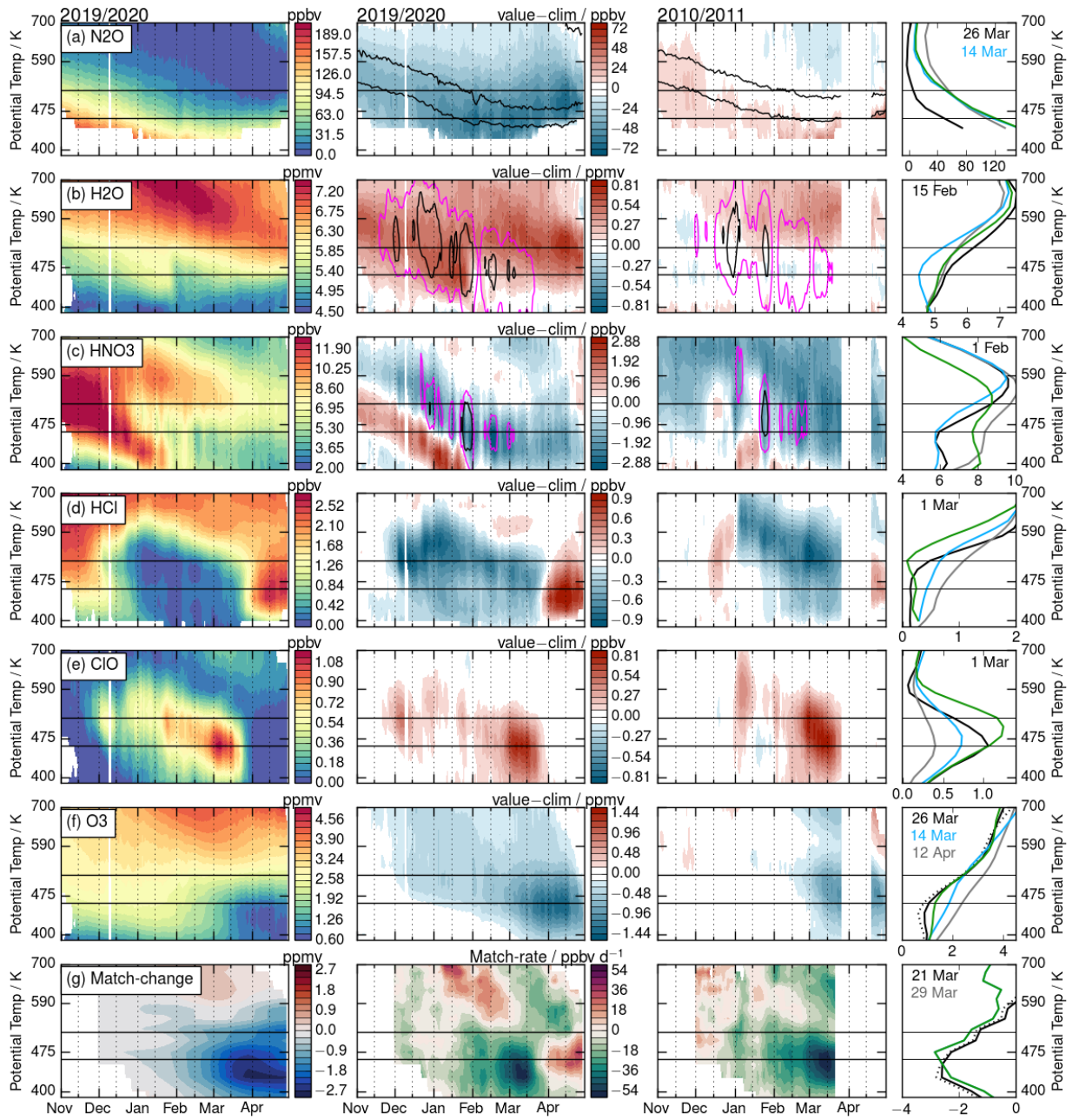
### 3 Summary and Conclusions

Figure 4 summarizes chemical processing and ozone loss at 460 and 520 K in 2019/2020 in comparison to the other winters observed by Aura MLS. Descent of unusually low N<sub>2</sub>O from the mid-stratosphere together with a well-isolated vortex resulted in smaller N<sub>2</sub>O abundances in the lower stratosphere in 2020 than in any previous winter observed by MLS. Depressed HNO<sub>3</sub> shows the onset of sequestration in PSCs in December; although the timing varied with altitude, the magnitude of the decrease was larger in 2019/2020. An abrupt drop in H<sub>2</sub>O in late January 2020 indicates sequestration of H<sub>2</sub>O in ice PSCs, but temperatures rose above the ice PSC threshold again too soon to produce vortex-wide dehydration of similar magnitude to that in 2016. Although H<sub>2</sub>O decreased over a small altitude range in 2020, at 460 K the drop during the coldest period was comparable to that in 2016.

Chlorine activation began slightly earlier in 2019 than in 2015 at 460 K and earlier than in 2010 at all levels. Previously, earliest strong Arctic chlorine activation was observed in 2012/2013, and the vortex was sufficiently exposed to sunlight for ClO to be elevated in late December (Manney et al., 2015). The timing of the HCl drop in 2019 was similar to that in 2012 at 460 K, but about ten days earlier at 520 K; at both levels highly elevated ClO was seen nearly two weeks earlier in 2019 than in 2012.

In 2011, chlorine deactivation occurred much later and followed a more Antarctic-like pattern than previously observed in the Arctic (e.g., Manney et al., 2011). The timing and pathway of chlorine deactivation in 2020 were even more similar to those in the Antarctic. Not only did ClO remain enhanced at 460 K as late as in 2011, but also HCl recovered much faster than usual and reached considerably higher values by mid-April than in 2011. In a typical Arctic spring, deactivation initially proceeds through reformation of ClONO<sub>2</sub>; however, several factors can shift Arctic chlorine partitioning toward HCl as in the Antarctic (e.g., Douglass et al., 1995; Santee et al., 2008). First, denitrification limits the availability of NO<sub>2</sub>, inhibiting combination with ClO to form ClONO<sub>2</sub>. In addition, low ozone and low temperatures together lead to preferential reformation of HCl (e.g., Douglass & Kawa, 1999). Thus HCl production was highly favored inside the persistently cold, strongly denitrified, and ozone-depleted Arctic vortex in spring 2020.

These conditions resulted in record-low Arctic O<sub>3</sub> values in spring 2020 at levels below ~500 K. Match estimates suggest more chemical loss in December 2019 through April 2020 than in 2010/2011 below ~460 K; peak losses were near 2.8 ppmv in each of these winters, but at lower altitude in 2020 than in 2011. While empirical O<sub>3</sub> loss estimates have large uncertainties (e.g., Griffin et al., 2019, also see SI), vortex-averaged



**Figure 3.** (a–f) Potential temperature/time sections of vortex averaged MLS species for 2019/2020 (left), and differences from 2004/2005–2019/2020 climatology for (center two columns) 2019/2020 and 2010/2011; right column: 2011 (green), 2016 (blue), and 2020 (black) profiles on extreme dates, and climatology (grey; for 2020 dates where those differ from other years). Black overlays in (a) show contours of N<sub>2</sub>O values that were at 540 and 620 K on 1 November. Overlays in (c) and (d) show area with MERRA-2 temperatures below NAT (magenta 3%, black 5%, of NH) and ice (magenta 1%, black 2%, of NH) PSC thresholds, respectively. (g) (left) Cumulative chemical O<sub>3</sub> change in 2020 from Match (see text and SI), (center two columns) Match rate of O<sub>3</sub> change in 2020 and 2011, and (right) profiles of cumulative O<sub>3</sub> change on 21 March 2020 (black) and 2011 (green), and 29 March 2020 (dotted line). Horizontal lines mark 520 and 460 K.

274 descent calculations using MLS N<sub>2</sub>O (overlaid lines/symbols in Fig. 4f,l) and using trajectory-  
 275 based descent rates (overlaid symbols in Fig. 4) (see SI for description of calculations)  
 276 give consistent results. They suggest that chemical loss between December and March  
 277 was very similar in the two winters, but that significant chemical loss occurred in Novem-  
 278 ber only in 2019. (As explained in the SI, the vortex-averaged descent methods give slightly  
 279 lower estimates than Match because they may be more affected by dilution of the chem-  
 280 ical loss signature near the vortex edge.) Record-low springtime O<sub>3</sub> at lower altitudes  
 281 in 2020 than in 2011 is consistent with evidence of record-low column O<sub>3</sub> and anoma-  
 282 lously high ultraviolet in 2020 (e.g., Bernhard et al., 2020). Large interannual variabil-  
 283 ity in meteorological conditions in the Arctic stratosphere (which led to the exception-  
 284 ally strong and long-lived polar vortex in 2019/2020) may yet result in more extreme Arc-  
 285 tic O<sub>3</sub> loss in future years while stratospheric chlorine loading remains high: For instance,  
 286 2015/2016 still stands out as the coldest Arctic winter with most denitrification and de-  
 287 hydration – if conditions such as those commenced as early in some future year and lasted  
 288 as late as in 2019/2020, and the vortex remained well-isolated, then greater O<sub>3</sub> deple-  
 289 tion could occur. This variability, coupled with likely effects of climate change, makes  
 290 comprehensive monitoring of polar processes such as that provided by Aura MLS (cur-  
 291 rently in the 16th year of a 5-year mission) an important priority moving forward.

## 292 Acknowledgments

293 We thank the Microwave Limb Sounder team at JPL, especially Brian Knosp, for MLS  
 294 retrieval processing, and computational, data processing, management, and analysis sup-  
 295 port; NASA’s GMAO for providing their assimilated data products; and Germar Bern-  
 296 hard, Vitali Fioletov, Jen-Uwe Grooß, Rolf Müller, and Ingo Wohltmann for helpful dis-  
 297 cussions. GLM and ZDL were partially supported by the JPL Microwave Limb Sounder  
 298 team under JPL subcontracts to NWRA. Work at the Jet Propulsion Laboratory, Cal-  
 299 ifornia Institute of Technology was done under contract with the National Aeronautics  
 300 and Space Administration. The datasets used here are publicly available:

- 301 • MERRA-2:  
 302 <https://disc.sci.gsfc.nasa.gov/uuu/datasets?keywords=%22MERRA-2%22>
- 303 • Aura MLS Level-2 and Level-3 data:  
 304 <https://disc.gsfc.nasa.gov/datasets?page=1&keywords=AURA%20MLS>

## 305 References

- 306 Bernhard, G. H., Fioletov, V. E., Grooß, J.-U., Ialongo, I., Johnsen, B., Lakkala, K.,  
 307 ... Svenby, T. (2020). *Record-breaking increases in Arctic solar ultraviolet ra-*  
 308 *diation caused by exceptionally large ozone depletion in 2020.* (to be submitted  
 309 to GRL for this special collection)
- 310 Butchart, N., & Remsberg, E. E. (1986). The area of the stratospheric polar vortex  
 311 as a diagnostic for tracer transport on an isentropic surface. *J. Atmos. Sci.*,  
 312 *43*, 1319–1339.
- 313 Douglass, A. R., & Kawa, S. R. (1999). Contrast between 1992 and 1997 high-  
 314 latitude spring Halogen Occultation Experiment observations of lower strato-  
 315 spheric HCl. *J. Geophys. Res.*, *104*(D15), 18,739–18,754.
- 316 Douglass, A. R., Schoeberl, M. R., Stolarski, R. S., Waters, J. W., III, J. M. R.,  
 317 Roche, A. E., & Massie, S. T. (1995). Interhemispheric differences in spring-  
 318 time production of HCl and ClONO<sub>2</sub> in the polar vortices. *J. Geophys. Res.*,  
 319 *100*, 13,967–13,978.
- 320 Gelaro, R., McCarty, W., Suárez, M. J., Todling, R., Molod, A., Takacs, L., ...  
 321 Zhao, B. (2017). The Modern-Era Retrospective Analysis for Research  
 322 and Applications, Version-2 (MERRA-2). *J. Clim.*, *30*, 5419–5454. doi:  
 323 doi:10.1175/JCLI-D-16-0758.1

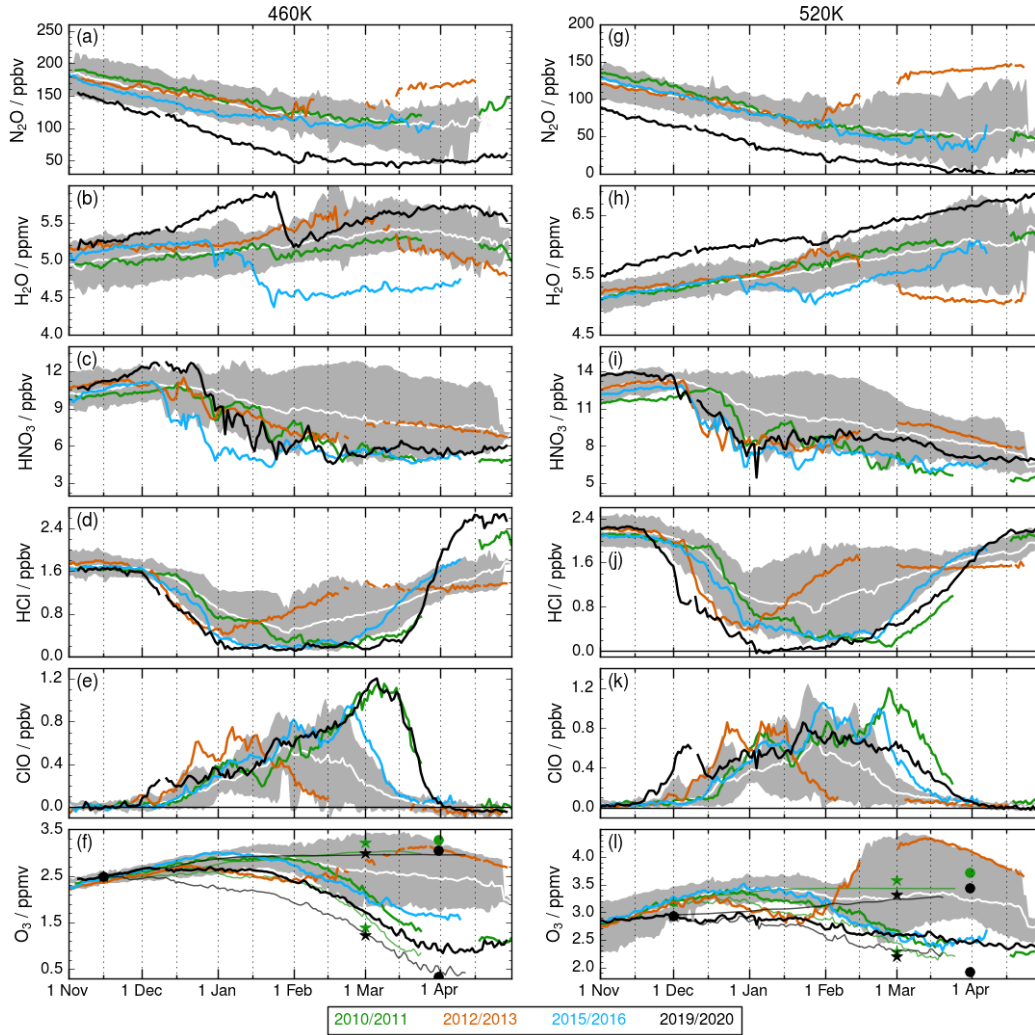


**Figure 4.** Vortex-averaged MLS trace gases for 2019/2020 (black), 2015/2016 (blue), 2012/2013 (orange), and 2010/2011 (green), at (a–f) 460 K and (g–l) 520 K. Grey envelope shows range of values for 2004/2005 through 2018/2019, excluding the highlighted years; white line shows mean for those years. Thin green and black lines in (f) and (l) show passive ozone (increasing lines) and calculated chemical loss in ozone estimated from MLS  $\text{N}_2\text{O}$  gradients (see SI) for 2011 and 2020, respectively; overlaid symbols shown passive ozone and chemical loss estimates (higher and lower values, respectively, on end dates) using trajectory-based descent estimates (see SI) with initial and final days shown as pairs of like symbols.

- 324 Griffin, D., Walker, K. A., Wohltmann, I., Dhomse, S. S., Rex, M., Chipperfield,  
325 M. P., ... Tarasick, D. (2019). Stratospheric ozone loss in the Arctic winters  
326 between 2005 and 2013 derived with ACE-FTS measurements. *Atmos. Chem.*  
327 *Phys.*, *19*(1), 577–601. Retrieved from [https://www.atmos-chem-phys.net/](https://www.atmos-chem-phys.net/19/577/2019/)  
328 [19/577/2019/](https://www.atmos-chem-phys.net/19/577/2019/) doi: 10.5194/acp-19-577-2019
- 329 Hanson, D., & Mauersberger, K. (1988). Laboratory studies of the nitric acid trihy-  
330 drate: Implications for the south polar stratosphere. *Geophys. Res. Lett.*, *15*,  
331 855–858.
- 332 Johansson, S., Santee, M. L., Grooß, J.-U., Höpfner, M., Braun, M., Friedl-  
333 Vallon, F., ... Woiwode, W. (2019). Unusual chlorine partitioning in the  
334 2015/16 Arctic winter lowermost stratosphere: observations and simula-  
335 tions. *Atmos. Chem. Phys.*, *19*(12), 8311–8338. Retrieved from [https://](https://www.atmos-chem-phys.net/19/8311/2019/)  
336 [www.atmos-chem-phys.net/19/8311/2019/](https://www.atmos-chem-phys.net/19/8311/2019/) doi: 10.5194/acp-19-8311-2019
- 337 Khosrawi, F., Kirner, O., Sinnhuber, B.-M., Johansson, S., Höpfner, M., Santee,  
338 M. L., ... Braesicke, P. (2017). Denitrification, dehydration and ozone loss  
339 during the 2015/2016 Arctic winter. *Atmos. Chem. Phys.*, *17*(21), 12893–  
340 12910. Retrieved from <https://www.atmos-chem-phys.net/17/12893/2017/>  
341 doi: 10.5194/acp-17-12893-2017
- 342 Lawrence, Z. D., & Manney, G. L. (2018). Characterizing stratospheric polar  
343 vortex variability with computer vision techniques. *Journal of Geophysical Re-*  
344 *search: Atmospheres*, *123*(3), 1510–1535. Retrieved from [http://dx.doi.org/](http://dx.doi.org/10.1002/2017JD027556)  
345 [10.1002/2017JD027556](http://dx.doi.org/10.1002/2017JD027556) (2017JD027556) doi: 10.1002/2017JD027556
- 346 Lawrence, Z. D., Manney, G. L., & Wargan, K. (2018). Reanalysis intercomparisons  
347 of stratospheric polar processing diagnostics. *Atmos. Chem. Phys.*, *18*, 13547–  
348 13579. doi: 10.5194/acp-18-13547-2018
- 349 Lawrence, Z. D., et al. (2020). *The remarkably strong Arctic stratospheric polar vor-*  
350 *tex of winter 2020: Ties to record-breaking Arctic oscillation and ozone loss.*  
351 (to be submitted to JGR for this special collection)
- 352 Livesey, N. J., Read, W. G., Wagner, P. A., Froidevaux, L., Lambert, A., Man-  
353 ney, G. L., ... Lay, R. R. (2020). *EOS MLS version 4.2x level 2 and 3*  
354 *data quality and description document* (Tech. Rep.). JPL. (Available from  
355 <http://mls.jpl.nasa.gov/>)
- 356 Livesey, N. J., Santee, M. L., & Manney, G. L. (2015). A Match-based approach to  
357 the estimation of polar stratospheric ozone loss using Aura Microwave Limb  
358 Sounder observations. *Atmos. Chem. Phys.*, *15*, 9945–9963.
- 359 Manney, G. L., & Lawrence, Z. D. (2016). The major stratospheric final warming  
360 in 2016: Dispersal of vortex air and termination of Arctic chemical ozone loss.  
361 *Atmos. Chem. Phys. Disc.*, *16*. Retrieved from [http://www.atmos-chem-phys-](http://www.atmos-chem-phys-discuss.net/acp-2016-633/)  
362 [discuss.net/acp-2016-633/](http://www.atmos-chem-phys-discuss.net/acp-2016-633/) doi: 10.5194/acp-2016-633
- 363 Manney, G. L., Lawrence, Z. D., Santee, M. L., Livesey, N. J., Lambert, A., & Pitts,  
364 M. C. (2015). Polar processing in a split vortex: Arctic ozone loss in early  
365 winter 2012/2013. *Atmos. Chem. Phys.*, *15*, 4973–5029.
- 366 Manney, G. L., Santee, M. L., Rex, M., Livesey, N. J., Pitts, M. C., Veefkind, P., ...  
367 Zinoviev, N. S. (2011). Unprecedented Arctic ozone loss in 2011. *Nature*, *478*,  
368 469–475.
- 369 Matthias, V., Dörnbrack, A., & Stober, G. (2016). The extraordinarily strong  
370 and cold polar vortex in the early northern winter 2015/2016. *Geophys. Res.*  
371 *Lett.*, *43*(23), 12,287–12,294. Retrieved from [http://dx.doi.org/10.1002/](http://dx.doi.org/10.1002/2016GL071676)  
372 [2016GL071676](http://dx.doi.org/10.1002/2016GL071676) (2016GL071676) doi: 10.1002/2016GL071676
- 373 Santee, M. L., MacKenzie, I. A., Manney, G. L., Chipperfield, M. P., Bernath, P. F.,  
374 Walker, K. A., ... Waters, J. W. (2008). A study of stratospheric chlorine  
375 partitioning based on new satellite measurements and modeling. *J. Geophys.*  
376 *Res.*, *113*. doi: 10.1029/2007JD009057
- 377 WMO. (2014). *Scientific assessment of ozone depletion: 2014*. Geneva, Switzerland:  
378 Global Ozone Res. and Monit. Proj. Rep. 55.